An experimental and numerical analysis of the dynamic variation of the angle of attack in a vertical-axis wind turbine

Melani, P. F.; Balduzzi, F.; Brandetti, L.; Ferreira, C. J.Simao; Bianchini, A.

DOI
10.1088/1742-6596/1618/5/052064

Publication date
2020

Document Version
Final published version

Published in
Journal of Physics: Conference Series

An experimental and numerical analysis of the dynamic variation of the angle of attack in a vertical-axis wind turbine

An experimental and numerical analysis of the dynamic variation of the angle of attack in a vertical-axis wind turbine

PF Melani[1], F Balduzzi[1], L Brandetti[2], CJ Simão Ferreira[2], A Bianchini[1]

[1] Department of Industrial Engineering, Università degli Studi di Firenze, Via di Santa Marta 3, 50139, Firenze, Italy.

[2] Delft University of Technology, Wind Energy, Kluyverweg 1, 2629HS Delft, The Netherlands.

Corresponding author: alessandro.bianchini@unifi.it

Abstract. Simulation methods ensuring a level of fidelity higher than that of the ubiquitous Blade Element Momentum theory are increasingly applied to VAWTs, ranging from Lifting-Line methods, to Actuator Line or Computational Fluid Dynamics (CFD). The inherent complexity of these machines, characterised by a continuous variation of the angle of attack during the cycloidal motion of the airfoils and the onset of many related unsteady phenomena, makes nonetheless a correct estimation of the actual aerodynamics extremely difficult. In particular, a better understanding of the actual angle of attack during the motion of a VAWT is pivotal to select the correct airfoil and functioning design conditions. Moving from this background, a high-fidelity unsteady CFD model of a 2-blade H-Darrieus rotor was developed and validated against unique experimental data collected using Particle Image Velocimetry (PIV). In order to reconstruct the AoA variation during one rotor revolution, three different methods – detailed in the study - were then applied to the computed CFD flow fields. The resulting AoA trends were combined with available blade forces data to assess the corresponding lift and drag coefficients over one rotor revolution and correlate them with the most evident flow macro-structures and with the onset of dynamic stall.

Keywords: Darrieus, VAWT, angle of attack, PIV, CFD

1. Introduction and objectives of the study

Applied research on Darrieus-type Vertical-Axis Wind Turbines (VAWTs) has been receiving a renewed attention for the last few years [1]. In particular, this technology is more often favorably associated to deep-sea, offshore floating installations due to the theoretical possibilities of shifting the generation system on the platform (so having a lower the center of mass), the absence of a yaw system, and the simple architecture [2]. Due to the lack of studies in the last thirty years of the 20th century, however, both the knowledge of involved physics and the state of development of existing simulation tools have fallen behind those for horizontal-axis machines. To this end, computational tools with a level of fidelity higher than that of the ubiquitous Blade Element Momentum (BEM) theory are increasingly applied to VAWTs, ranging from Lifting-Line methods, to Actuator Line ones or Computational Fluid

Dynamics (CFD) [3,4]. The greatest complexity in the analysis of Darrieus VAWTs relies in the continuous variation of the angle of attack during the cycloidal motion of the airfoils, going often much beyond the stall angle. This generates a variety of unsteady phenomena during the blade-flow interaction, making a correct estimation of the actual functioning conditions of the airfoils extremely difficult. Inter alia, dynamic stall strongly affects the performance of these machines, especially at medium-low tip-speed ratios (TSRs) [5]. A better understanding of the actual angle of attack (AoA) during the motion of a VAWT is however pivotal to select the correct airfoil and functioning conditions during the design and optimization phases.

Moving from this background, in the present study the unique experimental data collected using Particle Image Velocimetry (PIV) on a 2-blade H-Darrieus rotor in the TU Delft wind tunnel [6] were compared to high-fidelity, unsteady CFD simulations. Two operating conditions were tested, one in the unstable branch of the turbine characteristic curve (TSR=2) and one in the stable one (TSR=4.5). The main scopes of the comparison were to: a) compare the experimental and computed flow fields to assess the accuracy of the simulations and get an inner insight to the flow past rotating blades; b) reconstruct the AoA variation during the revolution and correlate it with the actual aerodynamic performance of the airfoils. For the latter purpose, three methods for the extrapolation of the AoA from the CFD flow field were selected: the *3-Points* [7], *Line Average* [8] and *Trajectory* [4] approaches. Originally developed for horizontal-axis machines, they were adapted to work with vertical-axis machines and then applied to the CFD data available for the TU Delft 2-blade rotor. The resulting AoA trends were combined with the CFD blade forces data to assess the corresponding lift and drag coefficients over one rotor revolution. The objective of this procedure was to understand how much the extracted blade loading data are sensitive to the choice of the AoA assessment method and thus to correlate the reconstructed AoA trends with the most evident flow macro-structures and with the onset of dynamic stall.

2. Methodology

2.1. Experiments

The experimental activity [6] has been performed in the Open Jet Facility (OJF), which is the closed-circuit, open-jet wind tunnel of the Delft University of Technology. The tested turbine model was a 2-blade (untwisted and untapered) H-Darrieus. The blade airfoil was a NACA0018, made of extruded aluminum section and having a chord of 0.06 m. Both the diameter and the height were equal to 1 m, thus leading to a turbine solidity of σ=0.12. Blades were hold in place by two straight struts per blade (NACA0030, chord 0.023 m). The velocity fields in the near wake of the turbine have been obtained by particle image velocimetry (PIV), adopted in a planar 2D–2C configuration for the horizontal plane at the turbine mid span and in a stereoscopic 2D–3C configuration for the measurements on the vertical planes. Further details on the experimental setup and the data acquisition/processing can be found in [6].

2.2. CFD simulations

Detailed unsteady Reynolds-Averaged Navier-Stokes (U-RANS) CFD simulations were carried out, based on a consolidated numerical approach developed by some of the authors [9], making use of the *k-ω SST* turbulence model, the coupled algorithm for pressure-velocity coupling, and the 2nd order upwind scheme for both RANS and turbulence equations. The sliding mesh technique was used to allow the rotation of the machine. The settings for convergence definition, maximum inner iterations and residuals were the same of [9]. The selected mesh refinement level and timestep were selected based on the experience of the authors on similar test cases and were verified to be compliant with the results of the sensitivity studies presented in [9] and particularly with the thresholds for the dimensionless vorticity and the Courant number proposed in [10].

2.3. AoA extraction methods

Different methods have been developed over the years for the extraction of the angle of attack on wind turbine blades, either from numerical (CFD) or experimental flow field data [7,8,11–15]. The majority

of these approaches, originally developed for horizontal-axis wind turbines (HAWTs), and only in some cases adapted to VAWTs [4], are based on the use of one or several sampling points to gather information about the velocity field around the airfoil. From such data, the so-called undisturbed velocity $\vec{V}$ is obtained, which is then combined with the turbine peripheral speed $\vec{U}$ to compute the angle of attack α on the blades:

$$\alpha = atan\left(\frac{-V_n}{V_t}\right) = atan\left(\frac{-V_x \sin\theta \quad {}_y \cos\theta}{-V_x \cos\theta - \ {}_y \sin\theta -}\right) \tag{1}$$

where Ω is the turbine rotational speed, R is the turbine radius and θ the blade instantaneous azimuthal position. Conventions and notations adopted for the current study are presented in figure 1.

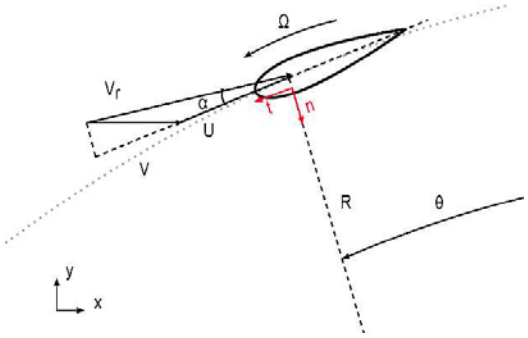

Figure 1. Conventions adopted for the present study

Although the arrangement of these points varies from one method to the other, it is always based on a two-dimensional modelling of the airfoil flow. As a consequence, they tend to lose coherence when the flow becomes inherently three-dimensional, i.e. near the blade tip or under massive flow separation [16]. If this represents a minor problem in HAWTs, where these issues are limited to the root and tip sections of the blade [11], it becomes of paramount importance when the focus is shifted on VAWTs. As anticipated in section 1, in fact the blades of these machines are usually subject to large AoA oscillations, which in some parts of the rotor revolution largely exceed the static stall limit. On top of that, the majority of small VAWTs are characterized by blades with low aspect ratio, so that the influence of the tip three-dimensional flow is extended to a major part of their span.

Starting from these considerations, the following approaches were selected from the literature and adapted for this study to work with VAWTs: the *3-Points*, *Line Average* and *Trajectory* methods.

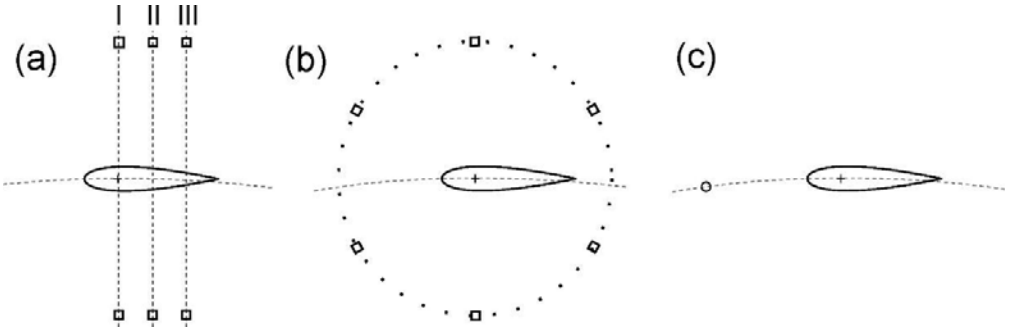

Figure 2. Position of the sampling points for the different methods: (a) 3-Points (b) Line average (c) Trajectory

2.3.1. 3-Points method. Originally developed by Rahimi et al. *[7,11]* to study the behaviour of horizontal-axis turbines in yawed flow conditions, the 3-Points method exploits six points in total, three on the suction side and three on the pressure side of the blade, to extract the AoA information from the flow field. As shown in figure 2a, for each side of the airfoil, the three points are located at a distance of 0.25c, 0.5c and 0.75c in the chord-wise direction starting from the leading edge, approximately 1c away from the blade aerodynamic centre in the normal direction.

The extraction of the AoA occurs in two main steps: 1) at each station along the chord, the average velocity vector is computed from the values sampled in the corresponding couple of points, via an *ad hoc* interpolation function; 2) the undisturbed velocity vector $\vec{V}$ is computed as the arithmetic average of the velocities coming from each station, as shown in equation (2):

$$\vec{V} = \frac{\vec{V}_I + \vec{V}_{II} + \vec{V}_{III}}{3} \tag{2}$$

According to [7,11], such strategy should be able to reduce the influence of bound circulation, together with the effects of upwash and downwash, over the measured incoming velocity. Furthermore, unlike other methods that have been developed for HAWTs, the 3-Point approach should be able to account for instantaneous velocity oscillations on the turbine blades, thus allowing one capturing also dynamic effects.

2.3.2. Line average method. The Line Average method (LineAve) has been introduced by Jost et al. [8], in the attempt of increasing the accuracy of previously available methods in capturing the effects of shed and trailing vorticity on the measured angle of attack on turbine blades. To this end, the undisturbed velocity $\vec{V}$ is computed as the integral average of the flow velocity field along a closed line around the airfoil (see figure 2b). According to the creators of the method, this sampling strategy should be able to completely remove the effect of bound circulation on the local inflow velocity, since in the averaging process the induced velocity components on any pair of opposite points on the closed path are levelled out, still accounting for the net distortion associated to trailing vorticity. This feature is particularly useful when modelling the flow around the blade tip. Nevertheless, since the method always includes the wake behind the profile, it might yield an unstable AoA trend when working in stalled conditions.

In the present study, in particular, it has been chosen to use a circular sampling line, centered in the aerodynamic center of the airfoil (assumed as the quarter-chord) and with a radius $r=1c$. According to [8], this configuration yields the best performance in terms of AoA sampling accuracy. Regarding the sampling resolution, two different configurations were tested, as shown in figure 1b: a low-resolution (points #, N=6) and high-resolution (points #, N=80) ones.

2.3.3. Trajectory method. The Trajectory method is an adaptation by Bianchini et al. [4] to VAWTs of the approach proposed by Shen et al. *[13]*, originally conceived for HAWTs. As shown in figure 2c, the local inflow velocity is sampled in a single monitor point on the trajectory outlined by the rotating blade, at a specified distance upstream its aerodynamic centre. In virtue of this strategy, the trajectory method is extremely easy to implement but, due to the lack of additional sampling points around the airfoil, it cannot provide any information about bound circulation and trailing vorticity. As a consequence, a theoretical model must be embedded into the method to account for the local flow deformation induced by these phenomena. More in detail, the vorticity distribution around the blade is modelled as a concentrated point vortex located in its aerodynamic centre and with a magnitude equal to the bound circulation Γ, that, according to the Kutta-Joukowksy theorem, can be computed as in equation 3:

$$\Gamma = \frac{L}{\rho V_r} \tag{3}$$

where L is the lift force on the blade, ρ is the freestream flow density and V_r is the relative air speed with respect to the airfoil. The induction exerted by the blade circulation on the flow at the sampling point is then computed via the Biot-Savart law (equation 4):

$$V_{in} = \frac{\Gamma}{2\pi d} \quad (4)$$

being d the distance between the sampling point and the blade aerodynamic center. The undisturbed velocity $\vec{V}$ is obtained by subtracting the induced velocity vector $\overrightarrow{V_{in}}$ from the one sampled in the monitoring point $\vec{V_s}$:

$$\vec{V} = \vec{V_s} - \vec{V_{in}} \quad (5)$$

Once $\vec{V}$ is known, the angle of attack α is computed from eq. 1. It must be noted that, since the lift force L is dependent on α, the procedure described so far must be applied in an iterative way. As demonstrated by Bianchini et al. [4], such correction strongly increases the robustness of the method, making the computed AoA almost independent from the sampling point position. Following the guidelines proposed in the same study, a distance of $1c$ between the sampling point and the blade quarter-chord is adopted for the current work.

3. Results

3.1. CFD model validation

The reliability of the developed CFD model was first verified by comparing the computed blade forces and flow fields surrounding the rotor with the ones available from experimental data (see section 2.1).

Figure 3 reports the comparison in terms of normal force F_N, in this case normalized over the freestream momentum $q_\infty=0.5\rho V_0^2$ and the turbine radius R, between numerical and experimental data over one rotor revolution. Fairly good agreement is apparent at both TSRs, especially in the upwind region ($0°\leq\theta\leq180°$), while in the downwind region ($0°\leq\theta\leq360°$), probably due to the disturbances associated to the blade shed vorticity and the presence of the shaft (see figure 4), the CFD curve tends to slightly deviate from experimental points. The same degree of matching, at least from a qualitative point of view, can be observed between the experimental and numerical flow fields shown in figure 4. Both the experimental axial velocity and vorticity fields are well reproduced by CFD, although the predicted wake seems narrower and less deflected than the measured one. Overall, the fair agreement between the two approaches justified the adoption of the developed tool for the analysis of the angle of attack on the rotor blades which is presented in section 3.2.

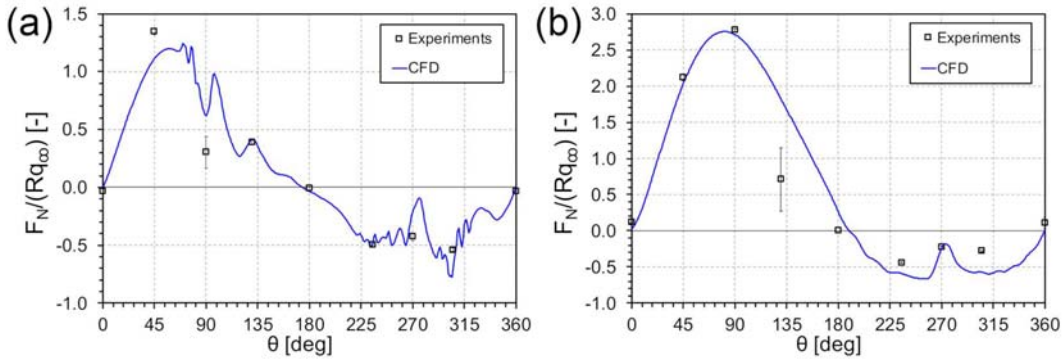

Figure 3. Comparison between experimental and CFD normal force azimuthal profile for: (a) TSR=2 (b) TSR=4.5

3.2. AoA trends

The different methods outlined in section 2.3 were applied to the CFD data, in order to reconstruct the corresponding AoA trend along one rotor revolution. The analysis was repeated for the same two turbine operating conditions, i.e. TSR=2 and TSR=4.5. The comparison is reported in figure 5.

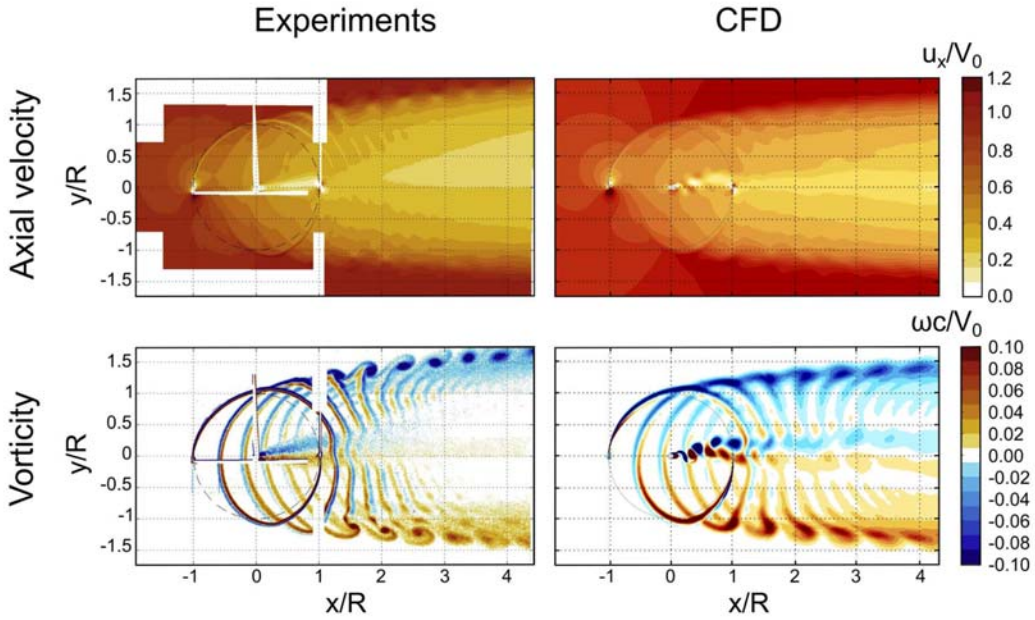

Figure 4. Comparison between experimental and CFD flow fields for TSR=4.5

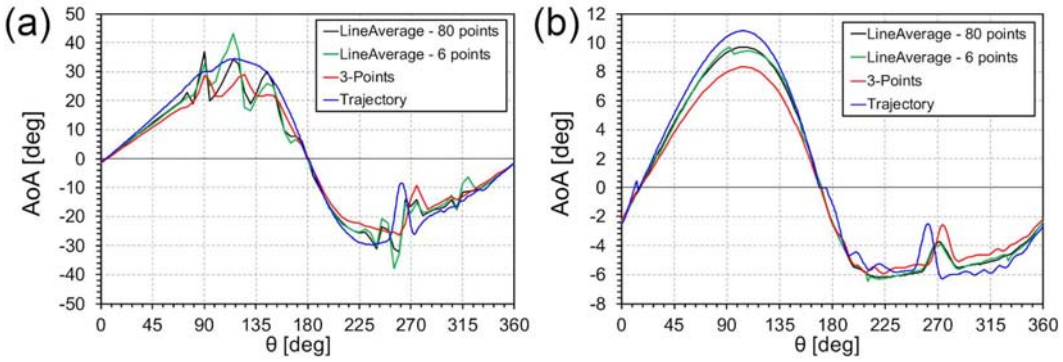

Figure 5. Comparison of the AoA azimuthal profiles obtained with different methods for: (a) TSR=2 (b) TSR=4.5

Upon examination of figure 5, fairly good agreement in terms of AoA between the tested methods is observed for low blade load conditions, i.e. for AoA ≤ 5°. Further increasing the angle of attack up to the static stall limit (AoA≈10°), the different curves start diverging one from the other. The overall deviation, however, remains limited to a few degrees.

Conversely, as the static stall limit is largely exceeded, the scattering between the various curves grows exponentially, leading to deviations larger than 10° in the most critical conditions (e.g. θ=100°, TSR=2). Such phenomenon, which has already been identified by Rahimi et al. [11], can be understood by recalling the theory underlying the formulation of the adopted methods.

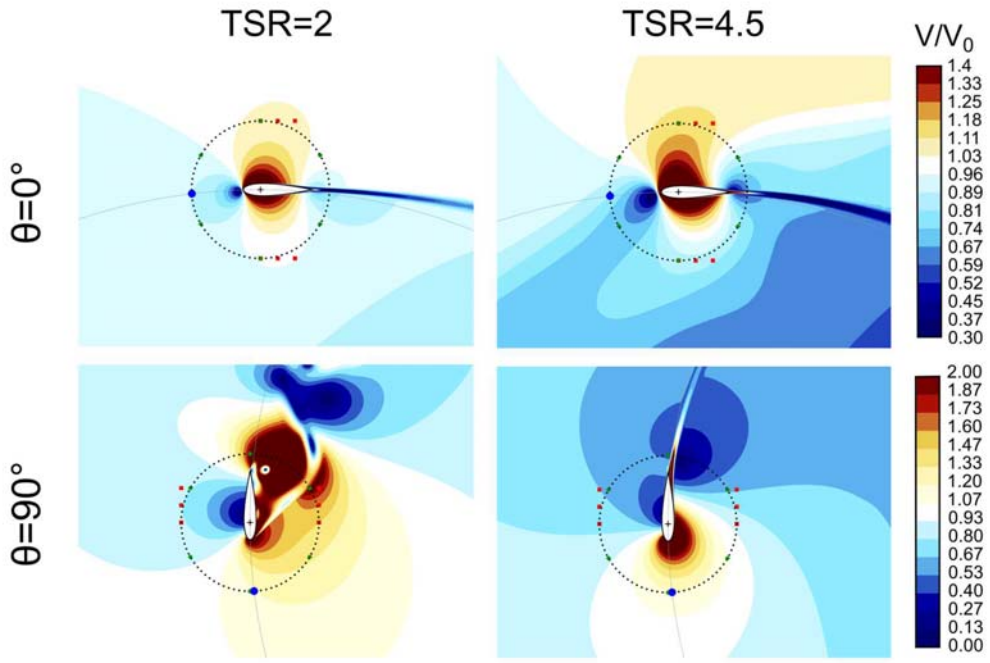

Figure 6. CFD velocity field data, normalized over the freestream velocity V_0

All of them are in fact based on the two-dimensional inviscid airfoil circulation theory [17], which assumes that the local flow around the blade can be interpreted as the superposition of the freestream and a free-vortex flow, which in turn depends on the intensity of the circulation Γ on the profile (see equations (3) and (4)). As long as this condition holds, i.e. viscous phenomena are confined to narrow region in the airfoil boundary layer and wake (*attached flow*), the different methods maintain a fair coherence one with the other. This occurs in a certain measure for TSR=4.5 (see figures 6 and 7b). On the contrary, when the static stall angle is exceeded, massive separation occurs on the airfoil surface. The circulation around the blade, as well as the overall vorticity distribution, are disrupted by the growth of the suction side boundary layer or, in case of dynamic stall, by the shedding of vortexes (see figure 7a). For this reason, when applied to critical rotor operation such as TSR=2, these methods become extremely sensitive to the arrangement of monitoring points.

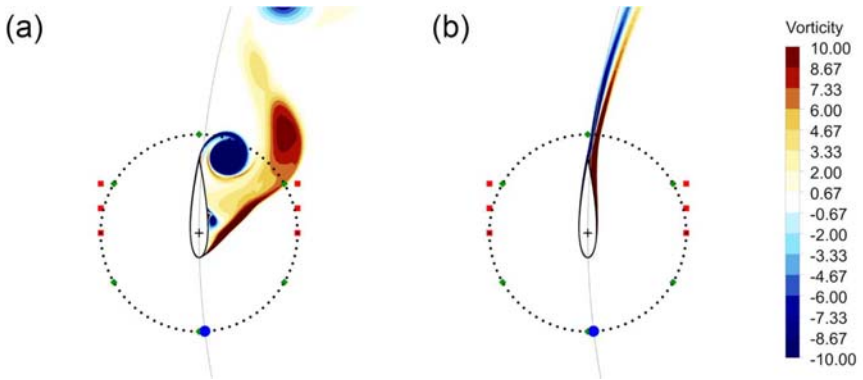

Figure 7. CFD vorticity field for: (a) TSR=2 (b) TSR=4.5

More in detail, the *Trajectory* approach is the one yielding the highest values of AoA over one revolution among the tested methods. Such phenomenon is particularly evident in the second quarter of the rotor revolution, i.e. between θ=60° and θ=150°, where the load experienced by the blades is maximum and, for the lower TSRs, massive flow separation occurs (see figure 6). The corresponding vortex shedding nonetheless is not captured by this approach, since the monitoring point is always positioned near the airfoil leading edge and thus no information about the flow pattern in the wake is provided. The resulting AoA profile is therefore smooth over the whole rotor revolution.

The AoA trend predicted by the *3-Points* method, on the other hand, presents severe oscillations in the deep stall region (see figure 5a). For some angular positions of the rotor, in fact some of the sampling points on the suction side fall in the vortexes shed by the blade. These unsteady flow structures, related to the dynamic stall phenomenon occurring at the most critical operating conditions such as TSR=2, are clearly visible in figure 7a. Extending the analysis to the whole rotor revolution, it can be seen from figure 5 how this approach yields the lowest AoA values among tested methods, for all operating conditions under consideration.

Finally, the *Line Average* method presents AoA trends, which are intermediate between those of the Trajectory and the 3-Points approaches. This phenomenon is probably related to the corresponding sampling strategy, which accounts for the flow pattern in both the leading edge and wake of the rotating blade (see figure 6). Nonetheless, the predicted AoA oscillations in the deep stall region (see figure 5a) are inherently more severe than those shown by the 3-Points method. In fact, the number of sampling points falling in the airfoil wake is overall higher than in the latter case, raising the weight of shed vorticity on the extracted AoA value. From figure 5, it can also be noted how, apart from a bunch of singularities, lowering the line resolution to N=6 has a very low influence on the predicted AoA trend.

3.3. C_L, C_D trends

Finally, the AoA trends reported in figure 5 were combined with the available CFD blade forces data (see figure 3) to assess the corresponding lift and drag coefficients over one rotor revolution.

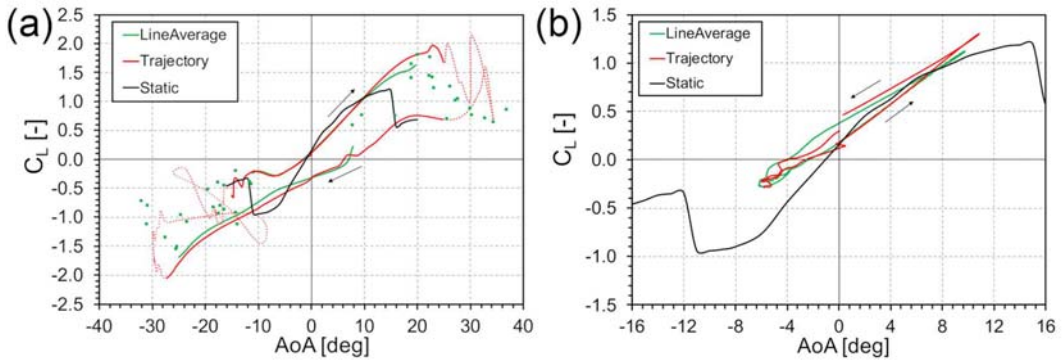

Figure 8. Comparison of the lift coefficient hysteresis loops obtained with different methods and static airfoil data for: (a) TSR=2 (b) TSR=4.5

In figure 8, the computed lift coefficient C_L (more significant than the drag one in VAWTs) is plotted against the corresponding angle of attack for the two operating conditions considered. The attended experimental static lift data for the airfoil at Re=150k [18], which is the average Reynolds number of the test turbine blade for TSR=4.5, are also reported as reference. It has to be noted that these data do not correspond to those of the "geometrical" NACA0018 airfoil, but to a virtual one cambered by the same revolution radius of the trajectory followed onboard the Darrieus turbine. This procedure was made in order to account for the *virtual camber* effect characterizing airfoils in cycloidal motion. In order to improve the readability of the graphs, the points that were considered to be unphysical, i.e. deriving

from bias of the AoA extraction method, or associated to dynamic effects, were represented as point clouds or discontinuous lines. This is the case for instance of the AoA values sampled with *Line Average* in the deep stall region (see figure 8a). For TSR=2, a heavily hysteretic behavior of the lift coefficient can be observed over the whole rotor revolution. Although at this operating condition the influence of the blade Reynolds number variation during rotation cannot be neglected, this phenomenon can be directly related to the onset of dynamic stall. As the AoA is raised beyond the static stall limit (AoA≈15°), the lift coefficient keeps increasing until reaching a maximum value, which is way higher than that allowed in static conditions. From a physical point of view, this corresponds to the formation of the leading edge vortex on the airfoil suction surface (see figure 7a) [19]. When such vortex is shed away from the profile, the lift coefficient drops down to values much lower than the static ones. This condition holds for the whole lower branch of the hysteresis loop, i.e. when the AoA is lowered until returning to the starting point. For TSR=4.5, although with a much lower extent than for TSR=2, an inherently hysteretic behavior of the lift coefficient is observed, as clearly visible in figure 8b. In this case though, since the AoA oscillation is contained in the static stall limit, such trend cannot be attributed to dynamic stall, but to an inherently inviscid unsteady phenomenon. During the pitch-down portion of the rotor upwind rotation in fact, a phase lag occurs between the flow incidence on the blades and their angular position, leading to an effective AoA which is higher than the nominal one [20]. The phenomena described so far are well captured by both the Line Average and Trajectory methodologies, which nonetheless deviate one from the other due to the scattering already encountered in the corresponding AoA trends (see section 3.2). Once again, such dispersion is quite limited in the pre-stall region, while it becomes extremely relevant in the deep stall one. As shown in figure 8, both the extension and the shape of the post-stall hysteresis loop change dramatically from one method to the other, making the selection of the proper approach crucial when analyzing highly unstable turbine operating conditions such as TSR=2.

4. Conclusions

The study presents a combined experimental and numerical approach applied to the analysis of the flow field surrounding a 2-blade H-Darrieus turbine in motion at different TSRs. An *ad hoc* unsteady CFD model of the test turbine has been developed and validated with PIV experimental data. The corresponding numerical flow fields have been then analyzed with three different methods, so that the angle of attack could be reconstructed along one rotor revolution. The resulting AoA trends showed a not negligible sensitivity with respect to the selected method, especially for AoA values approaching and exceeding the static stall limit. The maximum scattering has been observed for deep stall conditions, as the ones encountered for a large part of the rotor revolution at TSR=2. Such phenomenon is particularly pronounced for methods which sample the local velocity in the wake, such as the 3-Points and the Line Average ones, due to their interaction with the vorticity shed by the airfoil.

Eventually, the obtained AoA trends were combined with the available CFD blade forces data to assess the corresponding lift and drag coefficients over one rotor revolution. On one hand, this analysis highlighted the strict relationship between the AoA profile and the characteristics of the dynamic stall phenomenon experienced by the blades at the lower TSRs. Such evidence is also supported by the vortex structures observed in the CFD flow fields. On the other hand, it has been observed how the scattering characterizing the AoA trends obtained with the different methods is also reflected on the extracted blade loading profiles. Such uncertainty makes the choice of the proper method quite critical, especially when analyzing highly unstable turbine operating conditions such as TSR=2. As highlighted by this study however, no rigorous criterion is currently available to perform such selection. Therefore, further investigations must be carried out in the future, aimed at finding a proper methodology to validate the adopted AoA extraction method against available CFD and experimental data.

References

[1] Tjiu W, Marnoto T, Mat S, Ruslan M H and Sopian K 2015 Darrieus vertical axis wind turbine for power generation I: Assessment of Darrieus VAWT configurations *Renewable Energy* **75** 50–67

[2] Borg M, Shires A and Collu M 2014 Offshore floating vertical axis wind turbines, dynamics modelling state of the art. part I: Aerodynamics *Renewable and Sustainable Energy Reviews* **39** 1214–25
[3] Ferreira C S, Madsen H A, Barone M, Roscher B, Deglaire P and Arduin I 2014 Comparison of aerodynamic models for Vertical Axis Wind Turbines *Journal of Physics: Conference Series* **524** 012125
[4] Bianchini A, Balduzzi F, Ferrara G, Persico G, Dossena V and Ferrari L 2019 A critical analysis on low-order simulation models for darrieus vawts: How much do they pertain to the real flow? *Journal of Engineering for Gas Turbines and Power* **141** 011018
[5] Simão Ferreira C J, Van Zuijlen A, Bijl H, Van Bussel G and Van Kuik G 2010 Simulating dynamic stall in a two-dimensional vertical-axis wind turbine: Verification and validation with particle image velocimetry data *Wind Energy* **13** 1–17
[6] Tescione G, Ragni D, He C, Simão Ferreira C J and van Bussel G J W 2014 Near wake flow analysis of a vertical axis wind turbine by stereoscopic particle image velocimetry *Renewable Energy* **70** 47–61
[7] Rahimi H, Hartvelt M, Peinke J and Schepers J G 2016 Investigation of the current yaw engineering models for simulation of wind turbines in BEM and comparison with CFD and experiment *J. Phys.: Conf. Ser.* **753** 022016
[8] Jost E, Klein L, Leipprand H, Lutz T and Krämer E 2018 Extracting the angle of attack on rotor blades from CFD simulations *Wind Energy* **21** 807–22
[9] Balduzzi F, Bianchini A, Maleci R, Ferrara G and Ferrari L 2016 Critical issues in the CFD simulation of Darrieus wind turbines *Renewable Energy* **85** 419–35
[10] Balduzzi F, Bianchini A, Ferrara G and Ferrari L 2016 Dimensionless numbers for the assessment of mesh and timestep requirements in CFD simulations of Darrieus wind turbines *Energy* **97** 246-261
[11] Rahimi H, Schepers J G, Shen W Z, García N R, Schneider M S, Micallef D, Ferreira C J S, Jost E, Klein L and Herráez I 2018 Evaluation of different methods for determining the angle of attack on wind turbine blades with CFD results under axial inflow conditions *Renewable Energy* **125** 866–76
[12] Johansen J and Sørensen N 2004 Airfoil characteristics from 3D CFD rotor computations *Wind Energy* **7** 283–94
[13] Shen W Z, Hansen M and Sorensen J 2007 Determination of Angle of Attack (AOA) for Rotating Blades *Wind energy, proceedings of the euromech colloquium*
[14] Shen W Z, Hansen M O L and Sørensen J N 2009 Determination of the angle of attack on rotor blades *Wind Energy* **12** 91–8
[15] Herráez I, Daniele E and Schepers J G 2018 Extraction of the wake induction and angle of attack on rotating wind turbine blades from PIV and CFD results *Wind Energy Science* **3** 1–9
[16] Balduzzi F, Drofelnik J, Bianchini A, Ferrara G, Ferrari L and Campobasso M S 2017 Darrieus wind turbine blade unsteady aerodynamics: a three-dimensional Navier-Stokes CFD assessment *Energy* **128** 550–63
[17] Abbott I H A and Von Doenhoff A E 1959 *Theory of wing sections, including a summary of airfoil data* (New York: Dover Publications)
[18] Rainbird J M, Bianchini A, Balduzzi F, Peiró J, Graham J M R, Ferrara G and Ferrari L 2015 On the influence of virtual camber effect on airfoil polars for use in simulations of Darrieus wind turbines *Energy Conversion and Management* **106** 373–84
[19] Laneville A and Vittecoq P 1986 Dynamic Stall: The Case of the Vertical Axis Wind Turbine *Journal of Solar Energy Engineering* **108** 140–5
[20] Balduzzi F, Holst D, Melani P F, Wegner F, Nayeri C N, Ferrara G, Paschereit C O and Bianchini A 2020 Combined Numerical and Experimental Study on the Use of Gurney Flaps for the Performance Enhancement of NACA0021 Airfoil In Static and Dynamic Conditions *Proceedings of the ASME Turbo Expo 2020* London, UK